JOURNAL OF MECHANICAL ENGINEERING AND SCIENCES (JMES)
ISSN: 2289-4659 e-ISSN: 2231-8380
VOL. 15, ISSUE 2, 8169 – 8177
DOI: https://doi.org/10.15282/jmes.15.2.2021.16.0641

ORIGINAL ARTICLE

An experimental investigation on mechanical performances of 3D printed lightweight ABS pipes with different cellular wall thickness

B. Ergene[1], İ. Sekeroglu[2], Ç. Bolat[3] and B. Yalçın[4]

[1] Department of Mechanical Engineering, Faculty of Technology, Pamukkale University, 20180 Pamukkale, Denizli, Turkey
Phone: +905542814943; Fax: +902582964196
[2] Department of Research and Development, Şekeroğlu Chemistry and Plastic Industry and Trade I.C., 42050 Selçuklu, Konya, Turkey
[3] Department of Materials and Manufacturing, Faculty of Mechanical Engineering, Istanbul Technical University, 34437 Beyoğlu, Istanbul, Turkey
[4] Department of Mechanical Engineering, Faculty of Technology, Afyon Kocatepe University, 03200 Afyonkarahisar, Turkey

ABSTRACT – In recent years, cellular structures have attracted great deal of attention of many researchers due to their unique properties like exhibiting high strength at low density and great energy absorption. Also, the applications of cellular structures (or lattice structures) such as wing airfoil, tire, fiber and implant, are mainly used in aerospace, automotive, textile and biomedical industries respectively. In this investigation, the idea of using cellular structures in pipes made of acrylonitrile butadiene styrene (ABS) material was focused on and four different pipe types were designed as honeycomb structure model, straight rib pattern model, hybrid version of the first two models and fully solid model. Subsequently, these models were 3D printed by using FDM method and these lightweight pipes were subjected to compression tests in order to obtain stress-strain curves of these structures. Mechanical properties of lightweight pipes like elasticity modulus, specific modulus, compressive strength, specific compressive strength, absorbed energy and specific absorbed energy were calculated and compared to each other. Moreover, deformation modes were recorded during all compression tests and reported as well. The results showed that pipe models including lattice wall thickness could be preferred for the applications which don't require too high compressive strength and their specific energy absorption values were notably capable to compete with fully solid pipe structures. In particular, rib shape lattice structure had the highest elongation while the fully solid one possessed worst ductility. Lastly, it is pointed out that 3D printing method provides a great opportunity to have a foresight about production of uncommon parts by prototyping.

ARTICLE HISTORY
Received: 15th May 2020
Revised: 01st Nov 2020
Accepted:15th Dec 2020

KEYWORDS
Cellular structure;
3D printing;
mechanical performance;
energy absorption;
deformation mechanism

INTRODUCTION

Pipes are mostly used in drain, waste, vent systems as well as transporting various liquids that might be corrosive, flammable, explosives, volatile, reactive or sometimes hazardous to human health. Hence, right selection of pipe material can be seen as crucial when working conditions such as service temperature and pressure are evaluated [1]. Besides, other non-process factors that also considered during material selection are cost of material, availability and welding ability.

Nowadays, pipes are mainly manufactured from concrete [2], ceramic [3], metals [4, 5], glass [6] or plastics [7]. Especially, plastic materials are preferred due to their properties like light weight, chemical resistance, noncorrosive properties, and ease of making connections. Plastic materials like polyvinyl chloride (PVC), chlorinated polyvinyl chloride (CPVC), fiber reinforced plastic (FRP), reinforced polymer mortar (RPMP), polypropylene (PP), polyethylene (PE), cross-linked high-density polyethylene (PEX), polybutylene (PB), and acrylonitrile butadiene styrene (ABS), can be chosen as bulk materials of plastic pipes. Though both PVC and ABS pipes are resistant to most acids, alkalis, salt and they can be used above or below the ground, these kinds of polymers have their own advantageous and disadvantageous. For instance, it's easier to install ABS pipes than PVC pipes, since PVC pipes require a purple primer before each joint is glued together, and the joints must then be held together for 5 to 10 seconds for the glue to take hold [8].

Plastic pipes are generally extruded at desired outside diameters ranging 2 mm to 3000 mm due to the ease of handling the base materials. In particular, in drain, waste, vent and marine systems, the dimensions of plastic pipes can reach to length of 10 m and outside diameter of 3 m like shown in Figure 1 below. Apart from hot extrusion [9], pipes also can be produced with one of the most popular manufacturing methods is additive manufacturing [10].

Additive manufacturing, also known as 3D printing or rapid prototyping, is a novel manufacturing process benefiting from 3D model data and fabricates the desired product layer by layer. Therefore, this advanced manufacturing technology differs from the traditional manufacturing methods based on the principle of removing piece from the material like milling, turning or abrasive water jet cutting to obtain final product [11]. Most of the 3D printers used today work with fused deposition modelling (FDM) method which takes a place in one of the main seven additive manufacturing process methods called material extrusion.

*CORRESPONDING AUTHOR | B. Yalçın | ✉ bekiryalcin@aku.edu.tr

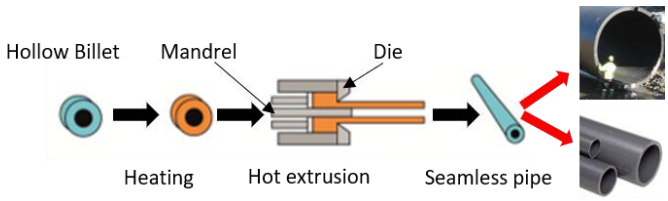

Figure 1. Manufacturing method of plastic pipes and various size products

A survey was done about 3D printing technology between 2014 and 2019 with 1300 respondents from all over the world and the results indicated that prototyping is the first reason of users with rate of over % 60 ahead of concept design/production and research & development [12]. In addition, prototyping provides a chance to foresee possible problems before manufacturing the products like dies, injection molds or the final products manufactured by hot extrusion or injection molding. As mentioned above, lately, researchers using 3D printers also focus on mechanical behaviors of novel structures like lattices [13] or hybrid composites [14] which can be manufactured by 3D printing methods without geometrical limits in order to minimize the waste material and production time.

In this study, by optimizing the wall thicknesses and geometries of pipes, new pipe models were designed by using cellular structures and the usability of these models was investigated in terms of compression behavior. If these designed prototype lightweight pipes provide sufficient mechanical properties, there will be less material consumption. Also, the difficulty in transporting large diameter pipes will reduce and the level of carbon dioxide arising from vehicles during the transfer of them will drop.

METHODS AND MATERIALS

Firstly, all pipe models with 150 mm length, 75 mm outer diameter and 64 mm inner diameter were designed. Then, in order to lighten the weight of the pipes, they were redesigned by optimizing the wall thickness (T) of all pipes except the fully solid pipe by using AutoCAD programme. Thus, three new models with different geometries at wall thickness section were obtained and T, t, Θ, h and l demonstrate the wall thickness, rib thickness, rib angle, height of honeycomb and length of honeycomb respectively (Figure 2(a)). In Figure 2(b-d), schematic view of redesigned lightweight pipes was given in order of rib pipe which containing only ribs, honeycomb pipe containing honeycombs and horizontal ribs connecting the honeycombs to each other and combination of first two pipes (hybrid pipe). Besides, fully solid pipe model was shown in Figure 2(e). Wall thickness (T) and rib thickness (t) was kept constant for all lightweight models and dimensions of honeycomb including Θ of 30^0 was assigned same for honeycomb and hybrid pipe models while designing and after manufacturing process all dimensions were measured ten times with Mitutoyo 500-182-30 digital caliper from various sections and average values were given in Table 1. In addition, measured results after manufacturing were compared with design dimensions and they seem quite similar with only maximum % 0.5 error for one side of honeycomb and % 1.7 error for rib thickness.

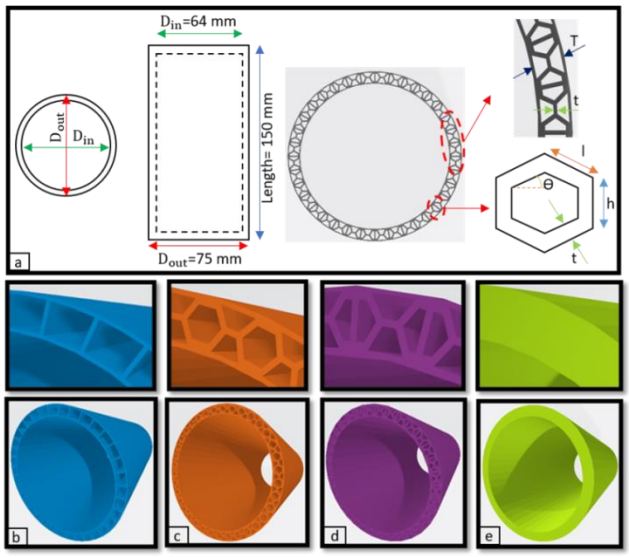

Figure 2. View of pipe dimensions and CAD models; (a) dimensions of pipes, (b) rib pipe, (c) honeycomb pipe, (d) hybrid pipe and (e) fully solid pipe

Table 1. Design and manufactured dimensions of pipes

	Rib Pipe		Honeycomb Pipe		Hybrid Pipe		Fully Solid Pipe	
DESIGN DIMENSIONS	Wall thickness (mm)	5.5	Wall thickness (mm)	5.5	Wall thickness (mm)	5.5	Wall thickness (mm)	5.5
	Rib thickness (mm)	0.59	Rib thickness (mm)	0.59	Rib thickness (mm)	0.59		
			One side of honeycomb, h=l (mm)	1.89	One side of honeycomb, h=l (mm)	1.89		
MANUFACTURING DIMENSIONS	Average Wall thickness (mm)	5.51	Average Wall thickness (mm)	5.50	Average Wall thickness (mm)	5.51	Average Wall thickness (mm)	5.5
	Average Rib thickness (mm)	0.58	Average Rib thickness (mm)	0.59	Average Rib thickness (mm)	0.59		
			Average one side of honeycomb, h=l (mm)	1.89	Average one side of honeycomb, h=l (mm)	1.90		

Designed lightweight pipe models shown in Figure 2(b-e) were additively manufactured from Zaxe black and blue ABS filaments whose material properties obtained from supplier information; filament diameter of 1.75 mm, density of 1.05 g/cm^3 , tensile strength of 47 MPa, tensile strain of 2.5%, flexural modulus of 2300 MPa, heated platform temperature of 80^{o}C-120^{o}C and melting temperature of 220^{o}C-250^{o}C were tabulated in Table 2.

Table 2. Material properties of ABS filament

Diameter (mm)	Density (g/cm^3)	Tensile strength (MPa)	Tensile strain (%)	Flexural modulus (MPa)	Heated platform temperature (^{0}C)	Melting temperature (^{0}C)
1.75	1.05	47	2.5	2300	80-120	220-250

Additively manufacturing process was conducted by using ZAXE X1+ mark FDM 3D Printer (Figure 3(c)) in Sekeroglu Company with process parameters that were tabulated in Table 3. The view of designed pipes can be seen at the slicing programme (Figure 3(a)) before manufacturing step and layer thickness and raft support was assigned as 0.2 mm and 0.8 mm respectively (Figure 3(b)). Additionally, no general support was needed because of building the parts through Z axis and infill ratio of parts was applied as fully solid. Besides, build plate with dimensions of 30x30x30 cm and extruder with diameter of 0.4 mm was heated to 100^{o}C and 240^{o}C. Lastly, 3D printed lightweight pipes which are ready for compression test were exhibited in Figure 3(d).

Table 3. 3D printing process parameters

Layer thickness (mm)	Build plate temperature (^{0}C)	Extruder temperature (^{0}C)	Infill ratio (%)	Raft support (mm)	General support (mm)
0.2	100	240	100	0.8	80-120

After the production of pipes, their weights were measured by using Precisa XB 220A SCS precision scales and weights of produced pipes were listed as 171.720 g, 86.808 g, 84.612 g and 44.74 g from large to small for fully solid, hybrid, honeycomb and rib pipes. Subsequently, manufactured lightweight ABS pipes were subjected to compression test between steel plates with 0.25 mm/min displacement. While compression test of pipes, deformation modes of pipes were recorded by video and then screenshot images were captured during test time from desired locations which exhibit how deformation occurred. Moreover, strain-strain curves were obtained from compression testing with the help of force-displacement data.

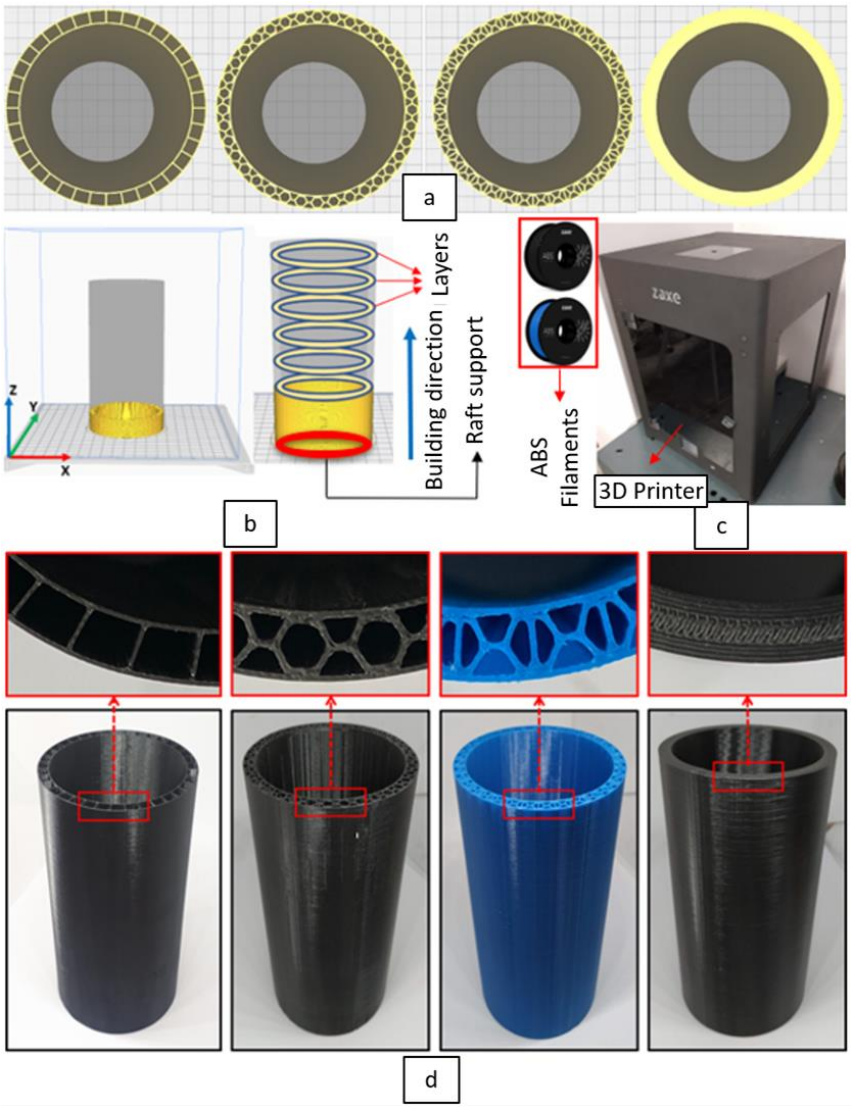

Figure 3. Manufacturing steps of pipes; (a) view of pipes in slicing programme before 3d printing process, (b) schematic view of building direction, layers and raft support, (c) 3D printer used and (d) 3D printed lightweight pipes

RESULTS

Mechanical Properties and Energy Absorption

Displacement-controlled uniaxial compression tests were conducted on additively manufactured samples using 50kN Shimadzu AG-IS uniaxial compression testing machine at the speed of 0.25 mm/min and force-displacement data produced from the compression tests were recorded by using Trapezium 2 software.

Typical stress-strain curves for all the different lightweight pipes were obtained by using force-displacement data and shown in Figure 4. By using the stress-strain curves, compressive strength, elasticity modulus, total energy absorption level and energy absorption capacity of lightweight pipes were calculated.

Likewise, specific compressive strength, specific modulus and specific absorbed energy were calculated by compressive strength, elasticity modulus and total energy absorbed energy values divided by multiplication of relative density and density of the bulk material (ABS). Hence, all calculated mechanical properties of pipes were tabulated in Table 4 below.

In Figure 5, mechanical properties of lightweight pipes were given in depth. According to Figure 5(a), fully solid pipe took the first place with compressive strength of 0.258 MPa and it was followed by honeycomb, hybrid and rib pipe with compressive strength values of 0.055 MPa, 0.054 MPa and 0.022 MPa respectively. It can be seen that honeycomb and hybrid pipe differ from rib pipe with presence of horizontal and angled ribs. Deformation mechanism of the horizontal and angled ribs exhibit that they support the vertical ribs and resist more till the fracture and so on honeycomb and hybrid pipes perform better compressive strength than rib pipe (Figure 6). Also, a similar trend was noticed when specific compressive strength values are examined too (Figure 5(b)). These consequences indicate that fully solid model pipe exhibits higher compressive strength than other types of pipe models, so fully solid pipe might be selected for applications requiring superior mechanical strength. On the other hand, if the specific strength values are taken into consideration, it

is clear that the difference observed between fully solid model and the others for compressive strength decreases owing to low relative density values of honeycomb, hybrid and rib models. Furthermore, elasticity modulus of lightweight pipes is presented in Figure 5(c) and the highest and lowest elasticity modulus of 2.822 MPa and 0.102 MPa were observed in order of fully solid sample and rib shaped sample. As for specific modulus, fully solid and honeycomb models displayed higher values (2958 Pa.m^3/kg and 2350.725 Pa.m^3/kg) although hybrid model and rib models had lower values (1918.009 Pa.m^3/kg, and 410.369 Pa.m^3/kg).

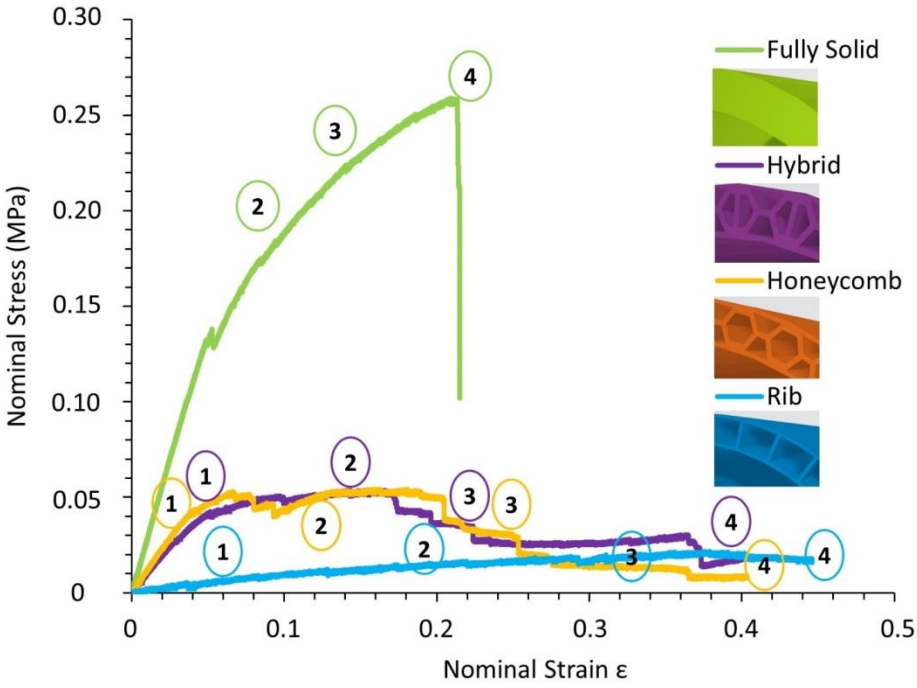

Figure 4. Stress-strain curves of lightweight pipes

Table 4. Mechanical properties of the samples under compression

Design	Compressive strength (MPa)	Specific Compressive Strength (Pa.m^3/kg)	Elasticity Modulus (MPa)	Specific Modulus (Pa.m^3/kg)	Energy absorbed (kJ/m^3)	Specific energy absorbed (J/kg)
Fully Solid Pipe	0.258	270.440	2.822	2958.071	37.895	39.722
Hybrid Pipe	0.054	111.970	0.925	1918.009	13.586	28.170
Honeycomb Pipe	0.055	117.004	1.105	2350.725	12.608	26.821
Rib Pipe	0.022	88.510	0.102	410.369	6.122	24.630

When Figure 5(e) and Figure 5(f) are evaluated, fully solid pipe got energy absorption of 37.895 kJ/m^3 and it is followed by hybrid pipe with 13.586 kJ/m^3, honeycomb pipe with 12.608 kJ/m^3 and rib pipe with 6.122 kJ/m^3. It can be emphasized that the presence of the vertical rib in hybrid pipe delayed the stress decrease (Figure 4) and improved the energy absorption when compared to honeycomb pipe. From Figure 5(e), it is correct to express that, maximum energy absorption capability difference was calculated between the fully solid pipe and rib shaped pipe (approximately 6.2 times). However, the lowest difference was found between hybrid and honeycomb pipes (approximately 1.07 times). On the other hand, when specific energy absorption capabilities were checked up on in Figure 5(f), the results approached to each other significantly with the effect of weight of pipes. Specific energy absorption values were determined 39.722 J/kg for fully solid, 28.170 J/kg for hybrid, 26.821 J/kg for honeycomb and lastly 24.630 J/kg for rib pipe. According to these results, it can be asserted that the difference recorded between the fully solid and rib pipes for energy absorption diminished from 6.2 times into 1.6 times if the specific energy absorption capacities were examined. In addition, it is known that the lattice structures are widely preferred in the applications of many sectors such as crash box in automotive [15], load-bearing parts of the wings in aircraft [16] and hip implant in biomedical [17] because of their high strength at low density and great energy absorption ability [18,19]. Similarly, experimentally obtained results from this study show that the unique idea of applying the lattice structures into the wall thickness of casual pipes have a remarkable potential. Moreover, using

less material while manufacturing will reduce the cost besides leading to an easier transportation and assembly of the huge pipes.

If the elongation values until the all pipe models were broken are analyzed, strain values of 0.446, 0.403, 0.401 and 0.215 were observed for rib, honeycomb, hybrid and fully solid respectively (Figure 4). According to the strain measurements, it is obvious that the rib shaped sample possessed the highest ductility compared to other designs. Hybrid and honeycomb models performed similar elongation behavior because of their similar structures and close relative density values. Nevertheless, the fully solid pipe exhibited worst ductility and reflected more brittle behavior owing to its high relative density and fill rate.

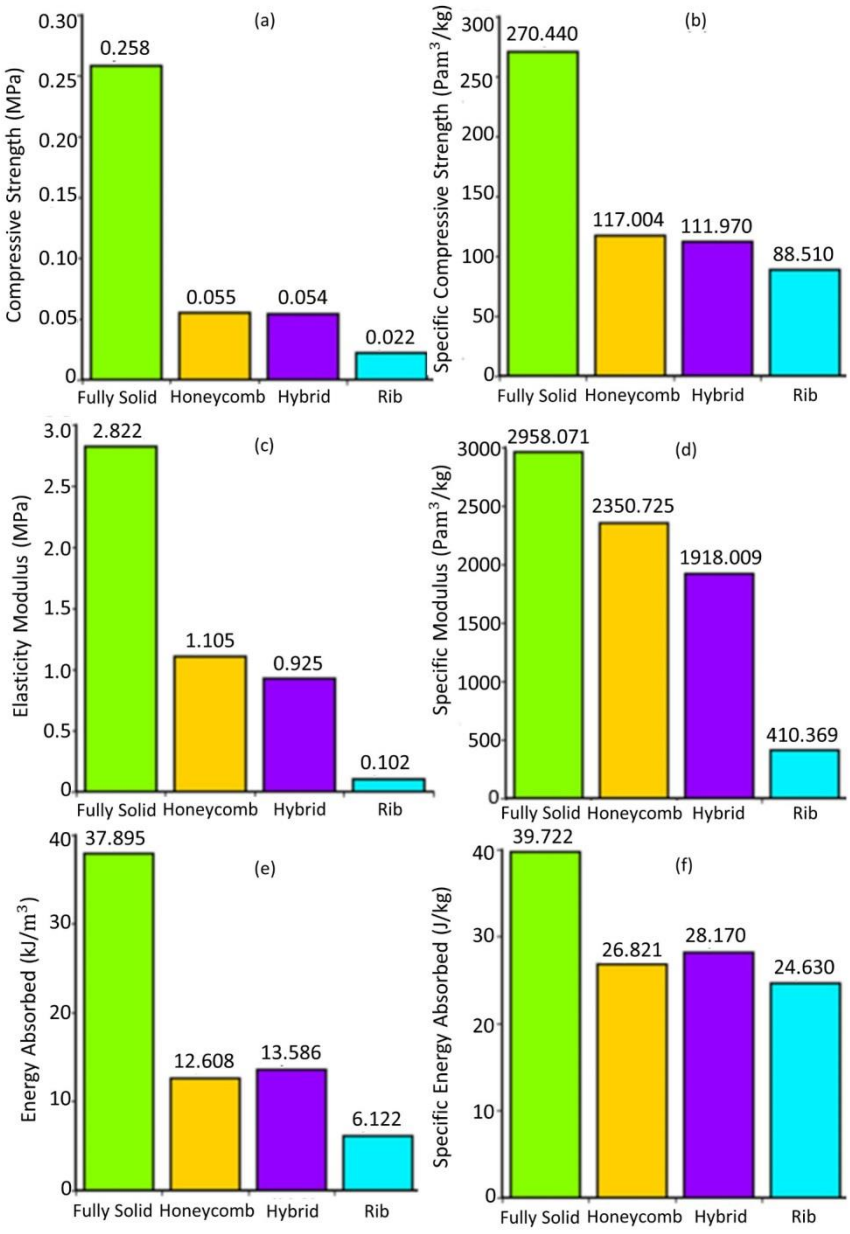

Figure 5. Mechanical properties of lightweight pipes; (a) compressive strength (MPa), (b) specific compressive strength (Pa.m^3/kg), (c) elasticity modulus (MPa), (d) specific modulus (Pa.m^3/kg), (e) absorbed energy (kJ/m^3) and (f) specific absorbed energy (J/kg)

Deformation Modes

Deformation modes of lightweight pipes at four different deformation points exhibited in the stress-strain curves besides their initial points are presented in Figure 6 with details. Moreover, Figure 7 demonstrates after deformation views of all four lightweight pipe models in detail. Firstly, when the rib shaped sample is evaluated, it can be interpreted that bending of the ribs began visibly and whole sample expanded horizontally in the first deformation point located at 0.06 strain in the stress-strain curve. Then, at the second deformation point, a collapse from top of the sample was observed and topmost ribs tried to resist against compression. After that, undermost and topmost ribs in the sample lined up in an

almost straight line and ribs at lower left corner started to go up while deforming at point 3 which took a place in 0.33 strain. Lastly, rising of ribs located at left lower corner went on and two ribs at that location and a rib at the left cracked in deformation point 4 around 0.45 strain. Detailed views of the damaged ribs can also be construed with by glancing at Figure 7. Basically, the structure of rib pipe showed quite ductile behavior under compression and that circumstance can also be observed by looking at after deformation images given in Figure 7.

Deformation of honeycomb structure was not similar to rib shaped one, though till first deformation point same deformation behavior like bending of honeycombs observed as well. At deformation point 2 (0.13 strain), honeycombs located top middle and bottom middle started to deform and approach to each other. Besides, top and bottom deformation lines occurred towards the back of sample. Then, these deformation lines became more visible, deformation of leftmost / rightmost honeycombs observed and great stress changes occurred at deformation point 3 (0.26 strain) which can be seen in stress-strain curve with details. At 0.4 strain (deformation point 4) sample cracked from four different corners which take places out of honeycombs. Additionally, leftmost honeycomb in sample cracked from rib besides region out of honeycomb (Figure 7).

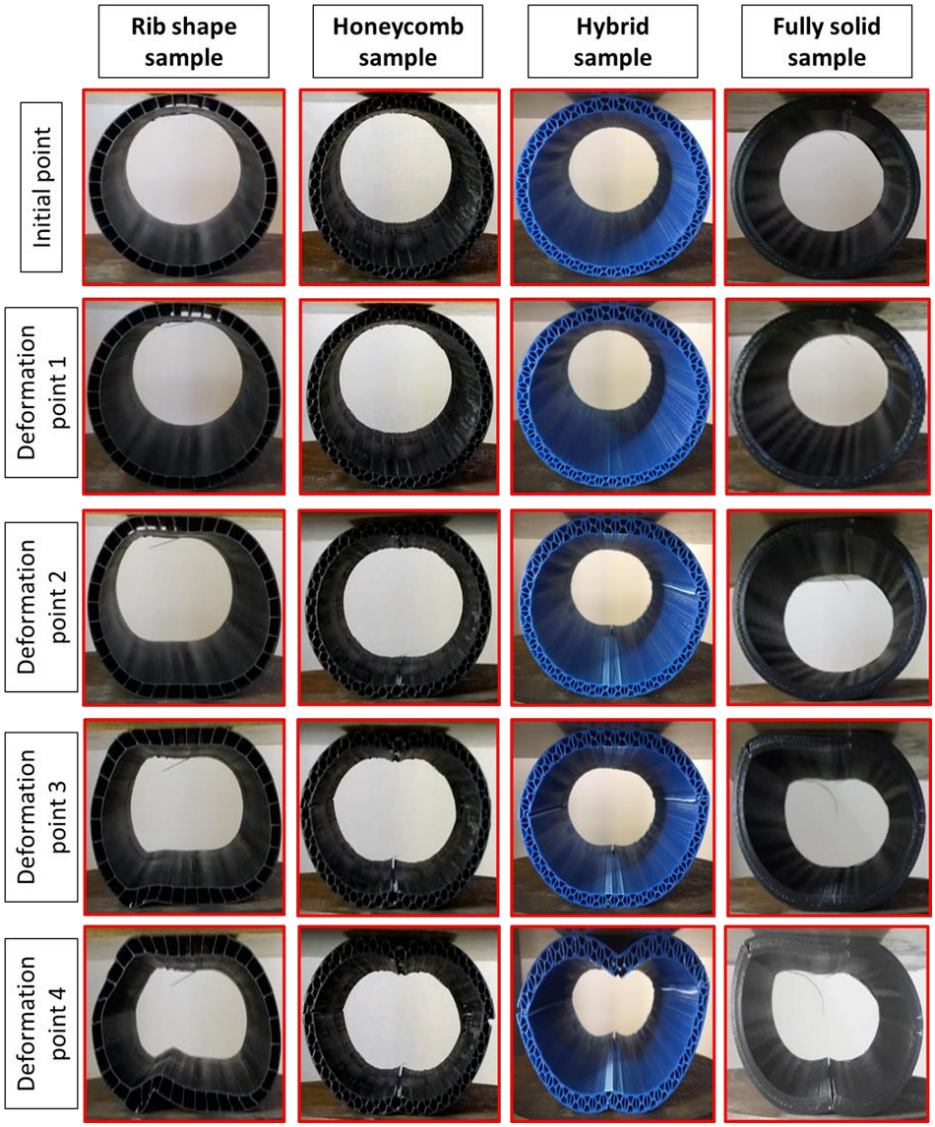

Figure 6. Deformation modes of lightweight pipes during compression test

Deformation behavior of hybrid sample was similar to honeycomb sample, but an important difference was understood at the same deformation points (points 1-4). The presence of vertical ribs in hybrid structure resisted against the compressive load and huge stress changes did not occur like in honeycomb model because of this reason and crack types included more ductile deformations when compared to honeycomb structure which does contain vertical ribs. From Figure 6 and Figure 7, all types of damage, such as long outer cracks, v-shaped ductile deformation and inner folds, can be observed depending on the compression load.

In the last stage, fully solid sample was subjected to compression testing in order to compare all samples with each other. At the first deformation point (0.05 strain), a stress change was visible and sample continued its contraction and expansion along compression axis and perpendicular axis respectively. At deformation point 2 (0.1 strain), deformation

locations became more apparent and they're followed by deformation point 3 (0.15 strain). Moreover, a crack formation at top left corner and a deformation line towards the back of sample was observed as well as other smaller crack formations located at various regions in sample depicted also in Figure 7 and crack propagation kept going till the last deformation point 4 (0.21 strain). Finally, stress rising stopped and the values dropped abruptly as seen from point 4 (Figure 4) since the outer crack at top left corner reached the inner section and an extra deep crack emerged at middle bottom side of the sample. Fully solid sample exhibited brittle fracture which differs from other samples tested. This significant result shows that though fully solid sample has higher compressive strength than other samples, it has a poor ability of strain because of displaying brittle behavior.

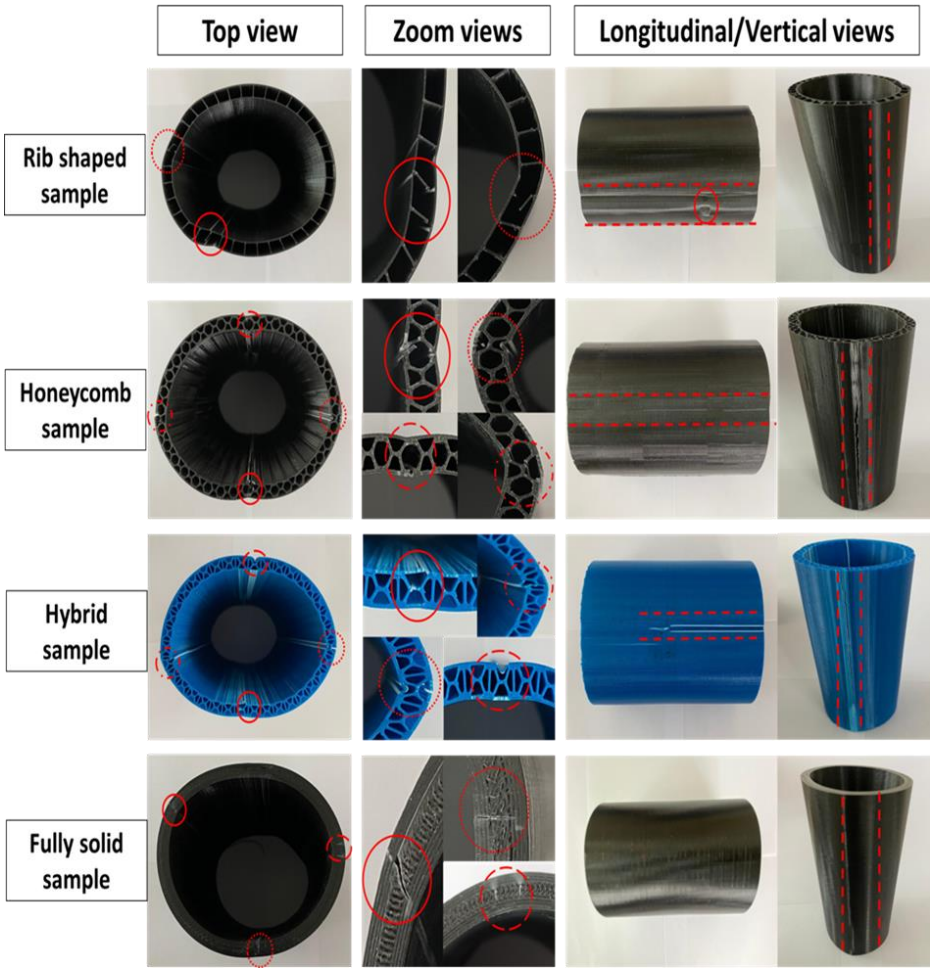

Figure 7. Views of deformed samples after compression test

CONCLUSIONS

In this paper, as a result of our efforts, the followings can be listed;

1) Additive manufacturing is a versatile fabrication technique and has also high potential for prototyping applications. In this context, different shapes of lightweight ABS pipe prototypes can be fabricated effectively by 3D printing technology. In case, the prototypes produced with additive manufacturing present positive outcomes like results of mechanical tests conducted in this study, suitable dies can be designed and manufactured in order to make mass production of these products by hot extrusion.

2) Fully solid pipe model has the highest compression strength and elasticity modulus values due to its high fill rate and total weight compared to other types.

3) Even though the highest energy absorption capacity is observed for fully solid pipe, if the specific values are taken into consideration, honeycomb, hybrid and rib shaped pipe models become also competitive depending on application conditions.

4) Rib shaped pipe model exhibits perfect ductility with the longest elongation value thanks to its low fill rate and perfectly fabricated rib structures. Following the rib pipe, honeycomb and hybrid models have also good elongation values, but the fully solid pipe performs worst.

5) Hybrid pipe model tends usually to show average properties in comparison with honeycomb and rib shaped pipes except for energy absorption capacity for which hybrid model is superior than the two.

6) At the initial stages of the compression, all samples act similarly. However, as long as the deformation continues, damage characteristics of them obviously differ from each other. From fully solid pipe model to the rib pipe, compression strength and elasticity modulus decrease, but the ductility increases sharply.

ACKNOWLEDGMENTS

The authors would like to acknowledge Şekeroğlu Chemistry-Plastic Industry and Trade I.C for research grants and funding.

REFERENCES

[1] N.A. Barton, T.S. Farewell, S.H. Hallett, T.F. Acland, "Improving pipe failure predictions: Factors affecting pipe failure in drinking water networks," *Water Research*, vol. 164, pp. 1-16, Nov. 2019, doi: 10.1016/j.watres.2019.114926

[2] Y. Sun, S. Hu, Y. Huang, X. Xue, "Analytical stress model for embedded bar-wrapped cylinder concrete pressure pipe under internal load," *Thin-Walled Structures*, vol. 149, Apr. 2020, doi: /10.1016/j.tws.2019.106540.

[3] Y. Li, L. Jiang, Q. Lu, P. Bai, B. Liu and J. Wang, "A study of ceramic-lined composite steel pipes prepared by SHS centrifugal-thermite process," *Science of Sintering*, vol. 48, no. 1, pp. 81-86, Jan. 2016, doi: 10.2298/SOS1601081L.

[4] H. Zhang, Y. Zhao, Y. Wang, H. Yu, C. Zhang, "Fabrication of nanostructure in inner-surface of AISI 304 stainless steel pipe with surface plastic deformation," *Journal of Materials Science & Technology*, vol. 34, no. 11, pp. 2125–2130, Nov. 2018, doi: 10.1016/j.jmst.2018.05.012.

[5] C.M.B. Martins, J.L. Moreira and J.I. Martins, "Corrosion in water supply pipe stainless steel 304 and a supply line of helium in stainless steel 316," *Engineering Failure Analysis*, vol. 39, pp. 65-71, Apr. 2014, doi: 10.1016/j.engfailanal.2014.01.017

[6] J. Kühnen, B. Song, D. Scarselli, N.B. Budanur, M. Riedl, A.P. Willis, M. Avila and B. Hof, "Destabilizing turbulence in pipe flow," *Nature Physics*, vol. 14, pp. 386–390, Jan. 2018, doi: 10.1038/s41567-017-0018-3.

[7] X. Zheng, X. Zhang, L. Ma, W. Wang and J. Yu, "Mechanical characterization of notched high density polyethylene (HDPE) pipe: Testing and prediction," *International Journal of Pressure Vessels and Piping*, vol. 173, pp. 11–19, June 2019, doi: 10.1016/j.ijpvp.2019.04.016

[8] M. L. Nayyar, *Piping handbook*. Mc-Graw Hill: Seventh Edition, pp. 1-2483, 2000.

[9] H.F. Giles Jr and J.R. Wagner Jr, *Extrusion: The definitive processing guide and handbook.* William Andrew: Second Edition, pp. 1-636, 2013.

[10] T. Sathish, M.D. Vijayakumar and A.K. Ayyangar, "Design and fabrication of industrial components using 3D printing," *Materialstoday:Proceedings*, vol. 5, no. 6, pp. 14489–14498, 2018.

[11] Epma, Introduction to Additive Manufacturing Technology: A guide for designers and engineers. Powder Metallurgy Association, 1st Edition, 2015. [Online], Available: https://futurerobotics.files.wordpress.com/2015/10/-epma_introduction_to_additive_manufacturing_technology.pdf

[12] The state of 3d printing, 2019 edition, 2019 [Online], Available: https://cdn2.hubspot.net/hubfs/5154612/downloads/-Sculpteo_The%20State%20of%203D%20Printing_2019.pdf

[13] Q. Wang, Z. Yang, Z. Lu and X. Li, "Mechanical responses of 3D cross-chiral auxetic materials under uniaxial compression," *Materials & Design*, vol. 186, pp. 1-12, Jan. 2020, doi: 10.1016/j.matdes.2019.108226

[14] L. Constantin, L. Fan, M. Pontoreau, F. Wang, B. Cui, J.L. Battaglia, J.F.Silvain and Y.F. Lu, " Additive manufacturing of copper/diamond composites for thermal management applications," *Manufacturing Letters*, vol. 24, pp. 61-66, Apr. 2020, doi: 10.1016/j.mfglet.2020.03.014

[15] S. Kazancı and J. Simpson, " Crushing investigation of crash boxes filled with honeycomb and re-entrant (auxetic) lattices", *Thin-Walled Structures*, vol. 150, 106676, 2020. doi: 10.1016/j.tws.2020.106676.

[16] P.R. Budarapu, S. Sastry, & R. Natarajan, "Design concepts of an aircraft wing: composite and morphing airfoil with auxetic structures". *Frontiers of Structural and Civil Engineering*, vol. 10, pp. 394-408, 2016. Doi: 10.1007/s11709-016-0352-z.

[17] H.M.A. Kolken, S. Janbaz, M.A. Sander, A. Leeflang, K. Lietaert, H. Weinansac and A.A. Zadpoora, "Rationally designed meta-implants: a combination of auxetic and conventional meta-biomaterials", *Materials Horizons*, vol. 5, no. 1, pp. 1–132, 2018. Doi: doi.org/10.1039/C7MH00699C.

[18] L.J. Gibson and M.F. Ashby, "Cellular Solids: Structure and Properties", *Cambridge University Press*, 1997. doi:10.1017/CBO9781139878326.

[19] B. Ergene and B. Yalçın, "Finite element analyzing of the effect of crack on mechanical behavior of honeycomb and re-entrant structures", *Journal of Polytechnic*, vol. 23, no. 4, pp. 1015-1025, 2020. Doi: 10.2339/politeknik.534103.